

Smith Predictor Based Control in Teleoperated Image-guided Beating-heart Surgery

Meaghan Bowthorpe, Mahdi Tavakoli, PhD, and Harald Becher, MD, PhD, FRCP, Robert Howe, PhD

Abstract—Surgery on a freely beating-heart is extremely difficult as the surgeon must perform the procedure while following the heart’s fast motion. However, by controlling a teleoperated robot to continuously follow the heart’s motion, the surgeon can operate on a seemingly stationary heart. The heart’s motion is calculated from ultrasound images and thus involves a non-negligible delay estimated to be 100 ms that, if not compensated for, can cause the robot end-effector (i.e., the surgical tool) to collide with and puncture the heart. This research proposes the use of a Smith predictor to compensate for this time delay. The results suggest that this improves heart motion tracking as the mean absolute error, the difference between the surgeon’s motion and the distance between the heart and surgical tool, and the mean integrated square error decreased.

I. INTRODUCTION

Beating-heart surgery is a super-human procedure as the surgeon must manually compensate for the heart’s fast motion, which has a velocity and an acceleration up to 210 mm/s and 3800 mm/s² respectively, while performing a surgical task [1]. Hence, surgical procedures are currently performed on an arrested heart or on a mechanically-stabilized heart [2].

In arrested-heart surgery, a heart-lung machine circulates the blood and ventilates the lungs; however, complications may occur when the heart is restarted. Other side effects include an increased risk of stroke [3] and/or long-term cognitive loss [4]. Conversely, mechanically-stabilized-heart surgery avoids these dangers but does not eliminate all of the heart’s motion. If a teleoperated robot could follow the heart’s beating motion, a surgeon could operate on a seemingly stationary heart, eliminating these side effects. Also, the normal heart motion would allow for *intra-operative* evaluation of a surgical procedure.

To develop such a surgical system, the point of interest (POI) on the heart must be tracked in real time. Various

This work was supported by NSERC and by an Alberta Innovates Graduate Student Scholarship awarded to M. Bowthorpe.

M. Bowthorpe is with the Department of Electrical and Computer Engineering, University of Alberta, Edmonton, AB T6G 2R3, Canada (e-mail: meaghan.bowthorpe@ualberta.ca)

M. Tavakoli, PhD, is with the Department of Electrical and Computer Engineering, University of Alberta, Edmonton, AB T6G 2R3, Canada (e-mail: mahdi.tavakoli@ualberta.ca)

H. Becher, MD, PhD, FRCP, is with the Faculty of Medicine and Mazankowski Heart Institute, University of Alberta, Edmonton, AB T6G 2R3, Canada (e-mail: haraldbecher@med.ualberta.ca)

R. D. Howe is with the Harvard School of Engineering and Applied Sciences, Cambridge, MA, 02138 USA, and also with the Harvard Massachusetts Institute of Technology Division of Health Sciences and Technology, Cambridge, MA, 02139 USA (e-mail: howe@seas.harvard.edu)

sensors such as force sensors measuring the heart’s motion through direct contact [5], high-frame-rate video cameras [6], or medical image (mainly ultrasound) scanners [7] can be used to obtain this motion. Medical image guidance was chosen as it can be used for both intracardiac and external procedures. However, acquiring and processing images inevitably introduces a non-negligible time delay. For instance, in a 3D ultrasound scanner, the frame rate can be as low as 18 Hz [8]. The subsequent processing increases the delay, which, if not compensated for, may cause the teleoperated robot end-effector (i.e., the surgical tool) to collide with and puncture the heart.

II. BACKGROUND

Prior art can be separated into two main categories: *Prediction algorithms*, which *feed-forward* an estimate of the heart’s future motion as the reference position for the teleoperated surgical robot controller, and *predictive controllers*, which account for the time delays in a *feedback* structure and are informed by the dynamic characteristics of the surgical robot. Table I categorizes the contributions of past research based on which control method was used, whether medical images were used to obtain the heart’s motion, and whether the surgical robot’s dynamics were considered.

A. Feedforward compensation of delay through prediction

Most past research involving feedforward compensation of delay through prediction neglects the surgical robot’s dynamics and does not include feedback control. A variety of methods for tracking the POI on the heart have been proposed. Yuen et al. compared the performance of three heart motion estimators where the heart motion was collected from ultrasound images [10]. These algorithms were designed to control a one-dimensional motion compensating *hand-held* tool for mitral valve repair [1]. The surgical device

TABLE I: The previous research has been divided into different categories based on its approach to heart motion tracking and control.

	Prediction or Predictive Control	Image-Based	Robot Dynamics
[1], [9]	Prediction	No	No
[6]	Predictive Control	No	Yes
[10]	Prediction	Yes	No
[11]	Prediction	No	Yes
[12]	Predictive Control	No	Yes
Proposed Method	Predictive Control	Yes	Yes

dynamics did not have to be considered as there was no dynamic effect intervening between the surgeon’s motion and the rigid tool’s motion in a hand-held device. In other words, in a hand-held rigid device, there is no difference between the reference motion commanded by the user holding the device and the actual motion experienced by the device end-effector. Clearly, unlike the hand-held device case, device dynamics do matter in a teleoperated device case, which is the focus of this paper. Franke et al. proposed the use of adaptive filters as they are capable of following a slowly varying heart rate [11]. Bebek and Cavusoglu employed the electrocardiogram (ECG) to synchronize the beginning of the actual and estimated heartbeats [9]. Both Franke et al. and Bebek and Cavusoglu captured the heart’s motion with sonomicrometry crystals sutured onto the heart, which is not practical during surgery.

B. Feedback compensation of delay through predictive control

Predictive controllers use the dynamic model of the robot in a feedback structure to account for the delay inherent in the measurement of heart motion. Ginhoux et al. compensated for the respiratory and the heart beat induced motions separately using a repetitive generalized predictive controller and frequency cancellation respectively [6], [12]. This method did take the robot’s dynamics into account, but did not address time delay compensation as a very high-frame-rate camera (500 Hz) was used to acquire the heart motion.

The research reported in this paper builds on the work done by Yuen et al. [10] for controlling a hand-held surgical tool, and takes the next logical step by introducing a predictive control approach that considers *both the time delay due to the image-based heart motion tracking and the teleoperated surgical robot’s dynamics in a feedback control structure*. We augment the feedback controller with a modified Smith predictor to ensure that the distance between the teleoperated robot and the heart follows the surgeon’s motion despite the time delays caused by medical image acquisition and processing. An estimate of the heart’s current motion is added to the system as an additional set point. As well, we do consider the difference in the sampling rates between the acquisition of ultrasound images and the surgical robot’s update rate.

This paper is organized as follows. Section III describes an application of beating-heart surgery. Section IV formulates the research problem. Section V discusses the Smith predictor and its implementation. Sections VI and VII highlight the simulation and the experimental results respectively. Finally, concluding remarks are presented in Section VIII.

III. A REPRESENTATIVE IMAGE-GUIDED PROCEDURE

While the image-based heart motion tracking can be procedure-specific, the Smith predictor based control method developed in this paper applies to any teleoperated surgery on the beating heart performed under medical image guidance.

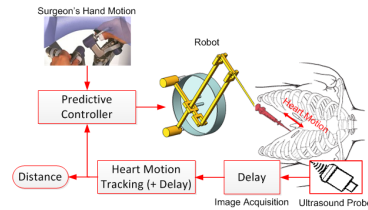


Fig. 1: The teleoperated image-guided beating-heart surgical setup for pericardiocentesis. The needle is inserted through the chest wall and into the pericardial sac to drain excess fluid but it should stop short of the heart tissue [13].

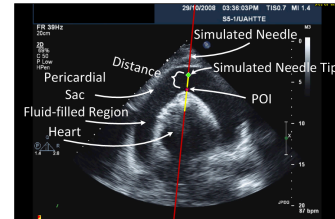


Fig. 2: A 2D ultrasound image from a patient who has a build-up of fluid in the pericardial sac. The red and yellow lines superimposed on the image represent the simulated needle’s position. The bright areas of the image are tissue and the dark areas are fluid-filled regions.

A. Pericardiocentesis

A procedure requiring one-dimensional tissue tracking is considered: pericardiocentesis, where a needle is inserted into the pericardial sac to drain the excess fluid that is constraining heart function. Currently, ultrasound images are used to find the optimal puncture site but, the needle is inserted with little or no intra-operative image guidance [14]. By using a heart motion-synchronized needle as shown in Fig. 1, the risk of puncturing a coronary artery could be greatly reduced.

B. Image-based tissue tracking

The goal of image-guided robotic assistance is to virtually stabilize the heart. To do so, the distance between the heart tissue and the needle tip is made to follow the surgeon’s motion. This distance is calculated from ultrasound images using the flashlight method developed by Novotny et al. [15]. Specifically, the axis of the needle, found using a Radon Transform modified for three dimensional data, is extended towards the heart tissue. The POI (the heart wall) is the closest change from a dark area (the fluid-filled region) to a light area (the tissue) beyond the needle tip, and is marked by the pink asterisk in Fig. 2. The movement of this tissue location is recorded as the heart’s displacement relative to the needle tip.

IV. PROBLEM FORMULATION

The aim of this research is to virtually stabilize the heart through the use of a teleoperated surgical robot. Because the surgical robot is teleoperated, its dynamics must be taken into account. In addition, the imaging delay must be compensated for while the heart’s repetitive motion, as well as the surgeon’s motions, are followed. A simple feedback control loop representing the unalterable “Physical system”, which includes the heart, surgical robot, and surgeon, and

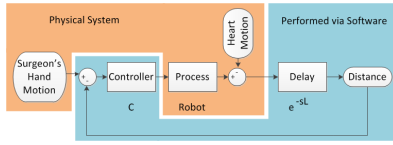


Fig. 3: The initial representation of the feedback controller that controls the robot's motion to follow the surgeon's motion.

the alterable part that is “Performed via Software” is shown in Fig. 3.

To begin, let us make the following observations:

- The heart motion is quasi-periodic,
- The last heart beat's motion can be extracted from the measured distance between the surgical tool and the heart.

Next, we will make the following assumptions:

- The surgical robot is a linear time-invariant system and has one degree of freedom,
- The time delay due to image acquisition/processing is constant and known,

A shortcoming of the system is that the distance data, calculated from the ultrasound images, arrives at a much lower sampling rate than the surgical robot's control update rate. Thus, the slowly sampled signal must be upsampled to take advantage of the surgical robot's capabilities. Furthermore, due to the delay, the system shown in Fig. 3 is unstable and/or has poor performance. To tackle this problem, we use a modified Smith predictor to compensate for this delay and to ensure that the system remains stable and retains the good performance it would have if the delay could be removed.

V. PROPOSED SMITH PREDICTOR BASED DESIGN

A Smith predictor is a predictive feedback controller that effectively separates the fixed delay from the feedback loop [16]. It does not limit one's choice of controller but the constant time delay and the model of the plant must be known. The Smith predictor ensures a control system retains the stability and good performance that it would have if the delay were not present. However, the delayed system will follow the input reference signal in the same manner as the non-delayed system except with a delay the length of the system's delay.

A. Controller Design

The output of the feedback loop in Fig. 3 follows the surgeon's motion, but not the heart's motion. Consequently, an estimate of the heart's motion is added – see Fig. 4a. Since the heart's motion is quasi-periodic, the measured motion from the past heart beat provides an estimate of the heart's motion in the current heart beat. An inner loop is added to help the robot follow the heart's (outdated) motion as well as the surgeon's (current) motion. In addition, four gain blocks, K_1 , K_2 , K_3 , and K_4 have been added: one for each feedback loop, one to scale the surgeon's motion, and one to scale the past heart motion. The controller, C , and these gains are designed based on the no-delay system – Fig. 4a. The transfer function between the three inputs: R : surgeon's

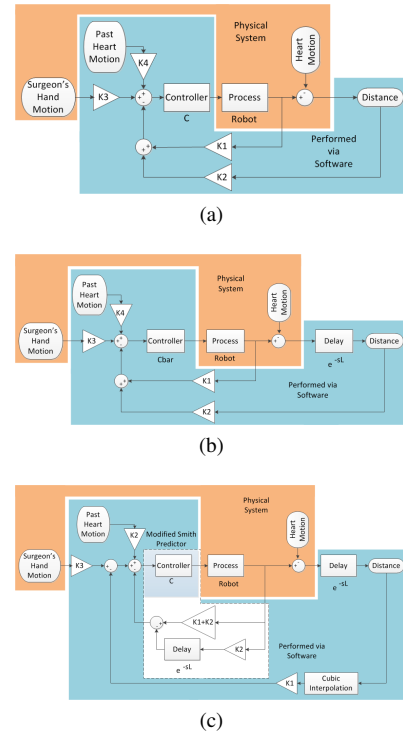


Fig. 4: The feedback controller designed to follow the surgeon's motion as well as the heart's motion with the added gain blocks, which increase the number of design parameters, is shown in a). The initial controller is then replaced by a Smith predictor in b). The complete control loop including the Smith predictor is shown in c).

motion, P : past heart motion, O : current heart motion, and the output: D : Distance between the needle tip and the heart wall is calculated.

$$D = \frac{(K_4 CG)P - (1 + CGK_1)Or + (CGK_3)R}{1 + CG(K_1 + K_2)} \quad (1)$$

The y-axis 1 joint of the Phantom Premium 1.5A robot, a haptic robot (Sensable group, now part of Geomagic, Wilmington, MA) was chosen as the surgical robot, G [17].

$$G = \frac{s^4 + 30.25s^3 + 2.923 \times 10^5 s^2 + 5.741 \times 10^5 s + 1.784 \times 10^{10}}{1.526s^4 + 233s^3 + 2.848 \times 10^5 s^2} \quad (2)$$

A proportional controller was chosen, $C = k$. The goal is to make the distance, D , follow the surgeon's motion, R . For this reason, the steady-state value of D is calculated when each of the inputs is a step function using the final value theorem, $d(\infty) = \lim_{s \rightarrow 0} sD(s)$ to calculate gains K_1 to K_4 .

The steady-state value of D is

$$\lim_{s \rightarrow 0} s \left(\frac{CG \frac{P}{s} - (1 + CGK_1) \frac{Or}{s} + CGK_3 \frac{R}{s}}{1 + CG(K_1 + K_2)} \right) \approx \frac{P - K_1 Or + K_3 R}{K_1 + K_2} \quad (3)$$

The distance, $d(\infty)$, given in (3), must equal the surgeon's motion, R_0 ; therefore the heart's motion, O_{r0} , and the past heart motion, P_0 , must cancel each other. Hence, K_1 must equal 1 as the heart's past motion, P_0 , should be

approximately equal to the heart's current motion Or_0 . Next, for the output to approach R_0 , K_3 must be equal to the sum of K_1 and K_2 .

The estimate of the heart's motion is based on the past cycle. However, the heart beat can change, so directly shifting the past heart motion will not provide a sufficient estimate. To improve this, an extended Kalman filter (EKF), as described by Yuen et al. [10], is used to calculate the current heart rate. From this rate, the length of time the past heart beat must be delayed to match the current heartbeat is calculated.

Finally, the multi-rate sampling issue is addressed by increasing the slow image acquisition sampling rate to the surgical robot's update rate using cubic interpolation. The cost is a longer delay, which can be added to the imaging delay and be compensated for by the Smith predictor.

B. Smith Predictor Design

Next, the new controller, \bar{C} , is designed to preserve the transfer function between the surgeon's motion, R , and the distance, D , when the time delay is present – see Fig. 4b. The transfer function between the surgeon's motion, R , and the distance, D , becomes

$$D = \frac{\bar{C}GK_3e^{-sL}}{1 + \bar{C}G(K_1 + K_2e^{-sL})}R, \quad (4)$$

where L is the length of the time delay and e^{-sL} represents a constant time delay. By equating the third term of the original transfer function in (1) multiplied by e^{-sL} to (4) and substituting in the values of K_1 , K_2 , and K_3 found previously, the Smith predictor \bar{C} is

$$\bar{C} = \frac{C}{1 + CGK_2(1 - e^{-sL})}. \quad (5)$$

The final control system model is shown in Fig. 4c, where \bar{C} has been replaced by (5) and the diagram has been simplified. It is important to note that because the surgical robot is physically separated from the delay, its model is not required as we have access to the surgical robot's position in real time (please note that the only measurement we cannot access in real time is the distance between the surgical robot and the heart). A slight disadvantage is that while the surgical robot will follow the heart motion on the fly, it will follow the surgeon's motions (in the ultrasound images) only after a delay. However, past research has demonstrated that a surgeon is capable of operating when there are delays up to 300 ms in transmission of motion commands to the teleoperated robot [18], thus an image acquisition delay of around 40 ms (25 Hz acquisition rate) is within the acceptable range.

VI. SIMULATION RESULTS

This proposed controller was simulated in Simulink. First, a heart motion signal is created by measuring the heart position in a sequence of ultrasound image frames of a beating heart lasting multiple heartbeats. The average of the heart position in these consecutive heart beats is calculated

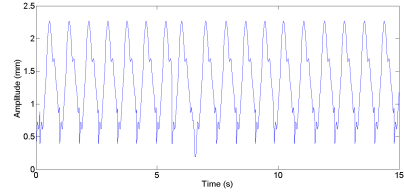


Fig. 5: The averaged distances between the heart wall and the stationary needle tip measured over multiple heart beats from a 2D ultrasound sequence. Each beat has been frequency matched to correspond to an actual clinical heart rate.

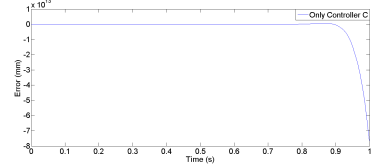


Fig. 6: The distance between the heart wall and the surgical instrument's tip when only a PID controller is used and the delay is present in the system. This case has unacceptable performance as the distance between the surgical tool and the heart wall continually increases.

to create the heart position over a single heart beat. This trajectory is then period matched to the heart rate of a clinical ECG from the MITBIH Database hosted by PhysioNet [19] and is shown in Fig. 5. A time delay of 100 ms and an acquisition rate of 25 Hz is used to simulate the delay and down sampling caused by the ultrasound image acquisition and processing. The four gain parameters K_1 - K_4 are set to 1, 9, 10, and 9 respectively. The performance of this system is evaluated by calculating the mean error between the surgeon's motion and the robot-heart distance – the distance between the needle and the heart – and the integrated squared error (ISE), $\frac{1}{n} \sum \varepsilon^2$, where ε is the difference between the surgeon's motion and the robot-heart distance and n is the number of data points.

To begin, the system is simulated without the Smith predictor or an estimate of the heart position. The robot-heart distance steadily increases as is shown in Fig. 6. Next, to determine the best possible performance, the delay is removed from the system, and hence the Smith predictor is also removed. The result is shown by the black line in Fig. 7a and the errors are given in line A of Table II. Then, the delay and the Smith predictor are returned to the system. The surgeon's motion is set to zero, the slow data was upsampled using cubic interpolation, and the estimated heart rate is updated by an EKF. The result is shown by the red line in Fig. 7a and the errors are given in line B of Table II. The effect of the surgeon's motion is now tested by using a chirp signal with an amplitude of 2 mm and a frequency ranging from 0.1 Hz to 5 Hz to represent it. The result is shown in Fig. 7b and the errors are given in line C of Table II. The errors are equal to those of the case when the surgeon's motion is removed, suggesting that the surgeon's motion does not affect the performance of the predictive control loop.

Finally, the effect of upsampling the slowly sampled data with cubic interpolation and of updating the length of the estimated past heart beat are studied. The chirp signal described above is included as the surgeon's motion in

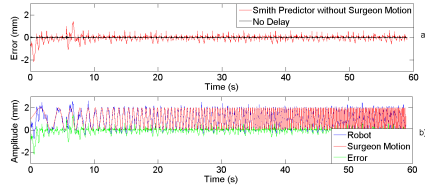


Fig. 7: The distance between the heart wall and the robot end effector when the surgeon’s motion is removed (a) and when it follows a chirp signal with a frequency ranging between 0.1 Hz and 2 Hz with an amplitude of 2 mm (b).

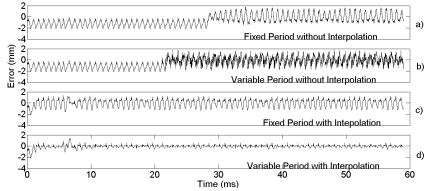


Fig. 8: A comparison of the error when ZOH interpolation a) and b) or cubic interpolation c) and d) is used and when the estimated heart beat length is updated b) and d) or not updated a) and c).

each of the following trials. The performance of each trial is compared based on the error calculated as the distance between the surgical tool’s motion and the surgeon’s motion. Ideally, these two trajectories should be identical. For the first two trials, a zero order hold (ZOH) is used to upsample the estimated heart motion and the distance between the surgical tool and the heart. In the first trial, the length of the past heart beat is set to 803 ms, the average heart beat length, and is kept constant throughout the trial - see Fig. 8a. In the second, the estimated heart rate is updated by an EKF - see Fig. 8b. The actual heart rate of the heart motion signal (see Fig. 5) changes throughout the trial. The mean error and mean ISE values are 0.95 mm and 1.12 mm^2 for the first trial and 0.82 mm and 0.98 mm^2 for the second trial. For the third and fourth trials, cubic interpolation is used to increase the sampling rate of the past heart motion and the distance between the needle and the heart wall. In the third trial the heart rate is not updated - see Fig. 8c; whereas in the fourth it is updated by an EKF - see Fig. 8d. The resulting mean error and mean ISE values are 0.57 mm and 0.42 mm^2 for the third trial and 0.15 mm and 0.07 mm^2 for the fourth trial. The best performance occurs when the estimated heart rate is updated and cubic interpolation is used.

TABLE II: A summary of the simulation results. (A) The Smith predictor and delay are removed and the surgeon’s motion is set to zero. (B)-(C): The Smith predictor and delay are included and the surgeon’s motion is (B) zero or (C) a chirp signal. The ratio between the error and the amplitude of the signal is given in brackets.

	Absolute Mean Error (mm)	Mean ISE (mm^2)
Simulation Results		
A	0.01 (0.48%)	2×10^{-4}
B	0.15 (7.2%)	0.07
C	0.15 (7.2%)	0.07

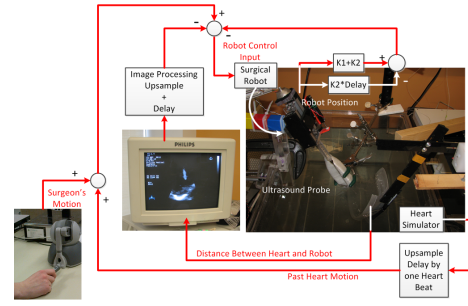


Fig. 9: The experimental setup. A linear voice coil motor actuates a needle which follows the heart simulator based on ultrasound guidance.

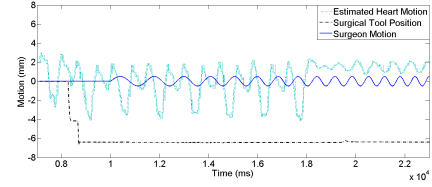


Fig. 10: The motion of the surgical tool tip and the corresponding distance between the simulated heart and the tool tip when no Smith predictor or estimated heart motion is used.

VII. EXPERIMENTAL RESULTS

Following the successful simulation of the system, preliminary experiments are performed with a teleoperated 1 DOF surgical tool under ultrasound guidance. The experimental setup - see Fig. 9 - includes a heart simulator, actuated by a DC motor, and a 1 DOF motion compensating surgical tool, actuated by a linear voice coil motor with a 20 mm trajectory (NCC20-18-02-1X, H2W Technologies Inc, Valencia CA). The position of the surgical tool and the heart simulator is measured by a linear potentiometer position sensor (A-MAC-B62, Midori America Corp, Fullerton CA). The motion of the entire system is captured by three dimensional ultrasound images acquired from a SONOS 7500 (Phillips Medical, Andover, MA). For a more detailed description see [15].

The trajectory of the point on the simulated heart pointed

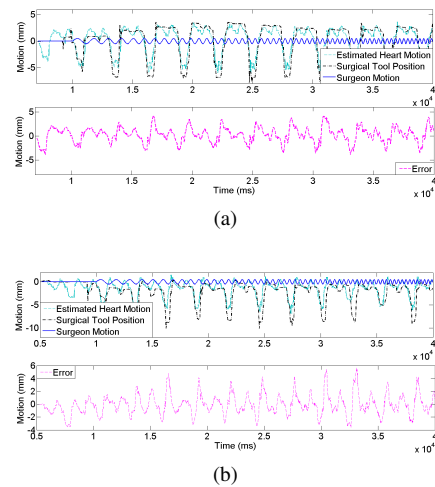


Fig. 11: The motion of the surgical tool tip and the corresponding distance between the simulated heart and the tool tip when (a) cubic interpolation and (b) ZOH interpolation is used.

TABLE III: A summary of the experimental results. The slow signal is upsampled via (A) cubic interpolation and (B) zero order hold. (C) The Smith predictor and heart motion estimation are removed. The ratio between the error and the amplitude of the signal is given in brackets.

	Absolute Mean Error (mm)	Mean ISE (mm ²)
Experimental Results	(delay included)	
A	1.24 (14%)	1.53
B	1.23 (15%)	1.51
C	4.31 (68%)	18.59

to by the surgical tool tip is obtained from ultrasound images and is shown by the light blue line in Figs. 10, 11a, and 11b. Two trials evaluating the effect of using interpolation are carried out. The total error in each trial is calculated from the ultrasound image and hence, is quite noisy. The estimated heart rate is not updated to reflect the current heart rate and is set to the average heart rate. A chirp signal with an amplitude of 2 mm centered at zero and a frequency ranging from 0.1 Hz to 5 Hz is used to represent the surgeon's motion.

First, the Smith predictor and estimated heart motion are removed from the system. The result is shown in Fig. 10 and the errors are given in line C of Table III. It is very poor, as expected. Next the Smith predictor and estimated heart motion are returned. The cubic interpolation case is shown in Fig. 11a and the ZOH interpolation case is shown in Fig. 11b. The error calculations use the interval where the surgical tool is being actuated. The errors are given in line A and line B of Table III for the cubic interpolation and ZOH cases, respectively. These errors are larger than those reported in the previous section, which is to be expected as the measurements are taken from noisy ultrasound images. However, the use of the Smith predictor greatly reduces the error as compared to when it is not present.

VIII. CONCLUDING REMARKS

This paper proposes a predictive feedback control system for image-guided teleoperated beating-heart surgery. This predictive control system ensures that the distance between the heart wall and the robot's end effector (i.e., surgical instrument) is commanded by the surgeon's motions that are input via a user interface. Ultrasound images are used to calculate the heart's motion because they are inexpensive to obtain, minimally invasive, and can visualize through blood, which is required for intracardiac surgery. Because the ultrasound images must be acquired and processed, a time delay is introduced into the control system, which if not compensated for, may cause the system to become unstable in the worst case or show unacceptable tracking errors in the mild case.

In this paper, a Smith predictor is added to the feedback control system to compensate for the above-mentioned delay. In this application, the Integrated Squared Error is greatly reduced in the simulations by incorporating a Smith predictor into the design. The low sampling rate of the ultrasound and the variable heart beat length are also accounted for. Future

work will focus on improving the prediction of the heart's motion by using past and current measurements.

REFERENCES

- [1] D. T. Kettler, R. D. Plowes, P. M. Novotny, N. V. Vasilyev, P. J. del Nido, and R. D. Howe, "An active motion compensation instrument for beating heart mitral valve surgery," in *IEEE/RSJ IROS*, 2007, pp. 1290–1295.
- [2] M. J. Mack, "Pro: beating-heart surgery for coronary revascularization: is it the most important development since the introduction of the heart-lung machine?" *Ann of Thorac Surg*, vol. 70, no. 5, pp. 1779–1781, 2000.
- [3] E. Bogatyrenko, U. D. Hanebeck, and G. Szabo, "Heart surface motion estimation framework for robotic surgery employing meshless methods," in *IEEE/RSJ IROS*, 2009, pp. 67–74.
- [4] M. F. Newman, J. L. Kirchner, B. Phillips-Bute, V. Gaver, H. Grocott, R. H. Jones, D. B. Mark, J. G. Reves, and J. A. Blumenthal, "Longitudinal assessment of neurocognitive function after coronary-artery bypass surgery," *New Engl J Med*, vol. 344, no. 6, pp. 395–402, 02/08 2001.
- [5] S. G. Yuen, D. P. Perrin, N. V. Vasilyev, P. J. del Nido, and R. D. Howe, "Force tracking with feed-forward motion estimation for beating heart surgery," *IEEE Trans. on Robotics*, vol. 26, no. 5, pp. 888–896, 2010.
- [6] R. Ginhoux, J. Gangloff, M. de Mathelin, L. Soler, M. M. A. Sanchez, and J. Marescaux, "Active filtering of physiological motion in robotized surgery using predictive control," *IEEE Trans. on Robotics*, vol. 21, no. 1, p. 67, 2005.
- [7] S. Yuen, S. Kesner, N. Vasilyev, P. Del Nido, and R. Howe, "3d ultrasound-guided motion compensation system for beating heart mitral valve repair," in *MICCAI 2008*. Springer Berlin / Heidelberg, 2008, vol. 5241, pp. 711–719.
- [8] S. Chandra, I. S. Salgo, L. Sugeng, L. Weinert, W. Tsang, M. Takeuchi, K. T. Spencer, A. O'Connor, M. Cardinale, S. Settlemyer, V. Mor-Avi, and R. M. Lang, "Characterization of degenerative mitral valve disease using morphologic analysis of real-time three-dimensional echocardiographic images / clinical perspective," *Circulation: Cardiovascular Imaging*, vol. 4, no. 1, pp. 24–32, 2011.
- [9] O. Bebek and M. C. Cavusoglu, "Intelligent control algorithms for robotic-assisted beating heart surgery," *IEEE Trans. on Robotics*, vol. 23, no. 3, pp. 468–480, 2007.
- [10] S. G. Yuen, P. M. Novotny, and R. D. Howe, "Quasiperiodic predictive filtering for robot-assisted beating heart surgery," in *IEEE ICRA 2008*, 2008, pp. 3875–3880.
- [11] T. J. Franke, O. Bebek, and M. C. Cavusoglu, "Improved prediction of heart motion using an adaptive filter for robot assisted beating heart surgery," in *IEEE/RSJ IROS*, 2007, pp. 509–515.
- [12] R. Ginhoux, J. A. Gangloff, M. F. de Mathelin, L. Soler, J. Leroy, and J. Marescaux, "Model predictive control for tracking of repetitive organ motions during teleoperated laparoscopic interventions," in *ECC*, 2003.
- [13] B. D. Hoit, "Pericarditis," September 2006. [Online]. Available: http://www.merckmanuals.com/professional/cardiovascular_disorders/pericarditis/pericarditis.html
- [14] M. Orsaneck, F. Bursi, P. W. OLeary, C. J. Bruce, L. J. Sinak, K. Chandrasekaran, and J. B. Seward, "Hand-carried ultrasound-guided pericardiocentesis and thoracentesis," *Journal of the American Society of Echocardiography*, vol. 16, no. 5, pp. 480–484, 5 2003.
- [15] P. M. Novotny, J. A. Stoll, P. E. Dupont, and R. D. Howe, "Real-time visual servoing of a robot using three-dimensional ultrasound," in *IEEE ICRA*, 2007, pp. 2655–2660.
- [16] O. J. M. Smith, "Closer control of loops with dead time," *Chemical Engineering Progress*, vol. 53, pp. 217–219, 1957.
- [17] M. Cavusoglu, D. Feygin, and F. Tendick, "A critical study of the mechanical and electrical properties of the phantom haptic interface and improvements for high-performance control," *Presence: Teleoperators and Virtual Environments*, no. 6, p. 555, 2002.
- [18] R. Rayman, S. Primak, R. Patel, M. Moallem, R. Morady, M. Tavakoli, V. Subotic, N. Galbraith, A. van Wynsberghe, and K. Croome, "Effects of latency on telesurgery: An experimental study," in *MICCAI*, vol. 3750, 2005, pp. 57–64.
- [19] A. L. Goldberger, L. A. N. Amaral, L. Glass, J. M. Hausdorff, P. C. Ivanov, R. G. Mark, J. E. Mietus, G. B. Moody, C.-K. Peng, and H. E. Stanley, "PhysioBank, PhysioToolkit, and PhysioNet: Components of a new research resource for complex physiologic signals," *Circulation*, vol. 101, no. 23, pp. e215–e220, 2000 (June 13).